

Identification of Lethal microRNAs Specific for Head and Neck Cancer

Marlon Lindenbergh-van der Plas¹, Sanne R. Martens-de Kemp¹, Michiel de Maaker¹, Wessel N. van Wieringen^{2,4}, Bauke Ylstra³, Reuven Agami⁵, Francesco Cerisoli⁶, C. René Leemans¹, Boudewijn J.M. Braakhuis¹, and Ruud H. Brakenhoff¹

Abstract

Purpose: The prognosis of head and neck squamous cell carcinomas (HNSCC) remains disappointing and the development of novel anti-cancer agents is urgently awaited. We identified by a functional genetic screen microRNAs that are selectively lethal for head and neck cancer cells but not for normal cells. We further investigated the genes targeted by these microRNAs.

Experimental Design: A retroviral expression library of human microRNAs was introduced in HNSCC cell lines and normal oropharyngeal keratinocytes to identify tumor-selective lethal microRNAs. Potential downstream gene targets of these microRNAs were identified by gene expression profiling and validated by functional assays.

Results: We identified six microRNAs that selectively inhibit proliferation of head and neck cancer cells. By gene expression profiling and 3'-untranslated region (UTR) luciferase reporter assays, we showed that the ataxia telangiectasia mutated (*ATM*) gene is a common target for at least two and likely three of these microRNAs. Specific inhibition of *ATM* resulted in a similar tumor-specific lethal effect, whereas the phenotype was reverted in rescue experiments.

Conclusions: These six microRNAs might be developed as novel anti-cancer agents and highlight *ATM* as an interesting novel therapeutic target for head and neck cancer. *Clin Cancer Res*; 19(20); 5647–57. ©2013 AACR.

Introduction

Head and neck squamous cell carcinoma (HNSCC) develops in the mucosal linings of the upper aerodigestive tract and contributes to approximately 5% of all cancers in the Western world (1, 2). Well-known risk factors are tobacco smoking, excessive consumption of alcohol containing beverages, and infection with the human papillomavirus (HPV; refs. 3–5). About one third of the patients present with early-stage tumors and receive single modality treatment, either surgery or radiotherapy. The 5-year survival rates for patients with early disease stages are more than 90%. Unfortunately the majority of patients with

HNSCC present with advanced disease stages. These patients are treated with either a combination of surgery and radiotherapy or chemoradiation, the concurrent application of systemic cisplatin chemotherapy combined with locoregional radiotherapy. Patients with advanced disease stages frequently develop locoregional recurrences, distant metastasis, and/or second primary tumors, which results in 5-year survival rates of less than 60% (1). Therefore, the development of novel anti-cancer agents to improve outcome is urgently awaited.

MicroRNAs (mi-RNAs) are about 22 nucleotides long, noncoding RNAs that are able to regulate the expression of multiple target genes (6). Classically, mi-RNAs regulate the expression of target genes through sequence-specific complementarity between the mi-RNA seed sequence and the 3' untranslated region (UTR) of the target mRNAs (7). Perfect complementarity between the mi-RNA and the mRNA will generally target the mRNA for degradation, whereas imperfect complementarity of the mi-RNA to the 3'UTR will preferentially repress mRNA translation (8). However, insights on the interaction of mi-RNA with their target genes evolve continuously. Through this regulation at the post-transcriptional level, mi-RNAs are able to modulate the expression of numerous genes simultaneously, thereby regulating individual signaling pathways at multiple levels (9).

Several studies have shown the importance of mi-RNAs in cancer, including HNSCCs. Altered mi-RNA expression profiles have been observed in both HNSCC cell lines and

Authors' Affiliations: Departments of ¹Otolaryngology/Head-Neck Surgery, ²Epidemiology and Biostatistics, and ³Pathology, VU University Medical Center; ⁴Department of Mathematics, VU University; ⁵Division of Gene Regulation, The Netherlands Cancer Institute, Amsterdam; and ⁶InterRNA Technologies BV, Utrecht, The Netherlands

Note: Supplementary data for this article are available at Clinical Cancer Research Online (<http://clincancerres.aacrjournals.org/>).

M.L. Lindenbergh-van der Plas, S.R. Martens-de Kemp, and R.H. Brakenhoff are listed as inventors on a PCT application.

Corresponding Author: Ruud H. Brakenhoff, Section Tumor Biology, Department of Otolaryngology/Head-Neck Surgery, VU University Medical Center, P.O. Box 7057, Amsterdam 1007 MB, The Netherlands. Phone: 31-20-44-40953; Fax: 31-20-44-43688; E-mail: rh.brakenhoff@vumc.nl

doi: 10.1158/1078-0432.CCR-12-2295

©2013 American Association for Cancer Research.

Translational Relevance

Head and neck cancer is a disease with grim prognosis, and novel treatments are urgently awaited. Here, we identified microRNAs that show a tumor-selective lethal effect and may serve as new therapeutic agents in head and neck cancer. Intratumoral injection in combination with electroporation of these microRNAs in head and neck tumors might be feasible, as access to the tumors is relatively easy. Importantly, we further show that the *ATM* gene is a target for some of these microRNAs and specific inhibitors of *ATM* showed a similar tumor-specific lethal effect. The application of *ATM*-directed drugs might be a very interesting approach for trials specifically focusing on head and neck cancer.

tumors when compared to the normal counterpart tissues (10, 11). The overexpression of miR-21 is described in many tumor types, including HNSCCs. Moreover, overexpression of miR-21 also increased with a higher grade of preneoplastic lesions during malignant progression (10). A number of these differentially expressed mi-RNAs were shown to be associated with poor prognosis, such as miR-21 and miR-211 (12, 13). Even more interestingly, recent studies have revealed that mi-RNAs may act as tumor suppressors by targeting oncogenes. For example, the miR-16 family inhibits cell-cycle progression and induces apoptosis via the silencing of *BCL2* (14), described in multiple tumor types, including HNSCCs. In a similar manner, ectopic expression of miR-181a resulted in decreased proliferation by targeting the oncogene *KRAS* (15).

In the present study, we examined the potential of mi-RNAs for treatment of HNSCCs. We hypothesized that mi-RNAs might cause tumor-specific cell death in HNSCCs by targeting genes that might show a synthetic lethal interaction with one or more inactivated cancer genes. Several tumor-suppressing routes are inactivated in HNSCCs among which the p53 and pRb pathways. Other genes or signaling routes may take over part of the lost functions and show a synthetic lethal interaction when inhibited (16). We used a human mi-RNA expression library in retroviral vectors to conduct a functional genetic screen to specifically identify mi-RNAs that cause cell death of tumor cells and not of primary keratinocytes. We further investigated, by expression array analysis, the target genes of these mi-RNAs as functional inhibition of the target genes may elicit the same lethal phenotype and could be conducted by small molecules.

Materials and Methods

Cell culture

Normal oral or oropharyngeal keratinocytes were isolated and cultured as previously described (17). Conditionally immortalized oropharyngeal keratinocytes (ciOKC) were generated by transformation of primary oropharyngeal keratinocytes with a temperature-sensitive SV40 large

T-antigen. Primary keratinocytes and ciOKCs were cultured in keratinocyte serum-free medium (KSFM; Invitrogen) supplemented with 0.1% bovine serum albumin, 25 mg bovine pituitary extract, 2.5 µg human recombinant EGF, 250 µg amphotericin B (MP Biomedicals) and 250 µg gentamycin (Sigma-Aldrich) at 32°C (18). VU-SCC-120, VU-SCC-OE, UM-SCC-6, SiHa, MCF7, HT29, U87, and Phoenix cells were cultured in Dulbecco's Modified Eagles' Medium (DMEM), 5% fetal calf serum, 2 mmol/L L-glutamine, 50 U/mL penicillin, and 50 µg/mL streptomycin at 37°C and 5% CO₂. The HNSCC cell lines used were all negative for the human papillomavirus and were sequenced for *TP53* mutations. Cell line UM-SCC-6 was *TP53* wild-type, VU-SCC-120 contained 2 missense mutations (c.181_182CG>TT and c.527G>A) and VU-SCC-OE a truncating deletion (c.11_919del). Cell lines are authenticated regularly by their morphologic characteristics and analysis of *TP53* mutations and genetic markers.

Functional screen of human mi-RNA library

Amphotropic retroviral supernatants were produced for 370 annotated and putative mi-RNAs included in the human mi-RNA expression library (mi-R-Lib) with miR-Vec-Ctrl (scrambled sequence) as negative control (18, 19). The conditionally immortalized oropharyngeal keratinocytes were used for screening experiments as described previously (18). ciOKC cells and VU-SCC-120 cells (HNSCC cell line previously described as 93VU120; ref. 20) were transduced for 24 hours (VU-SCC-120) or at 2 following days for 4 hours (ciOKC) in the presence of 3 µg/mL polybrene (Sigma-Aldrich). After 48 hours, the cells were subjected to blasticidin selection. For ciOKC, this was 2 days of 4 µg/mL and subsequently 5 days of 8 µg/mL blasticidin (Sigma-Aldrich). For VU-SCC-120, the selection was conducted with 10 µg/mL for 4 days. For the initial screen, cell survival was assessed by visual inspection when the negative control (miR-Vec-Ctrl) had reached 100% confluency and expressed as estimated percentage of the control (Supplementary Information). For subsequent validation experiments, cell viability was quantified using the CellTiter-Blue Cell Viability Assay (Promega). The conversion of resazurin to resorufin was measured using the Infinite 200 plate reader (Tecan Group Ltd.).

RNA isolation from formalin-fixed, paraffin-embedded tissue

Normal oropharyngeal mucosa was derived from 3 formalin-fixed, paraffin-embedded (FFPE) specimens from patients who underwent uvulopalatopharyngoplasty. In addition, FFPE tumor biopsies were obtained from 5 patients with HNSCCs. The mucosal epithelium was microdissected from sections of the uvula specimen as previously described (21). Likewise, neoplastic areas were microdissected from tumor samples. Microdissected tissues were treated with 1 mg/mL of proteinase K for 17 hours at 56°C in buffer containing 100 mmol/L Tris-HCl (pH 9.0), 10 mmol/L NaCl, 1% SDS, and 5 mmol/L EDTA (pH 8.2). Nucleic acids were isolated by phenol/chloroform

extraction and precipitated by sodium acetate and ethanol according to standard protocols using glycogen as carrier. After the nucleic acids were washed with 70% ethanol, they were redissolved in RNase-free water.

Lentiviral short hairpin RNA ATM transduction

Lentiviral vectors with short hairpin RNA (shRNA) sequences targeting *ATM* transcripts were obtained from the MISSION short-hairpin library of The RNAi Consortium (Sigma-Aldrich) that is available at VU University Medical Center. Viral supernatants were produced by cotransfection of HEK293T cells using FuGENE 6 (Roche Diagnostics) with the pLKO.1 short-hairpin vector together with the packaging and envelop vectors. Both ciOKC and VU-SCC-120 (HNSCC cell line) were transduced with lentiviruses at 2 following days for 4 hours in the presence of 3 µg/mL polybrene (Sigma-Aldrich). In total 48 hours after transduction, cells were subjected to puromycin selection. For ciOKC, this was 2 days of 5 µg/mL and subsequently 5 days of 10 µg/mL puromycin (Sigma-Aldrich), and for VU-SCC-120, the selection was conducted with 1 µg/mL for 7 days.

Quantitative reverse transcription PCR

Total RNA was isolated using the mirVana mi-RNA Isolation Kit (Ambion) according to the instructions of the manufacturer with the only modification that columns were eluted with 2 × 25 µL elution buffer. Expression of hsa-miR-181a, hsa-miR-323, hsa-miR-326, hsa-miR-342, hsa-miR-345, and hsa-miR-371 was analyzed by TaqMan microRNA assays following the instructions of the manufacturer (Applied Biosystems). *ATM* expression was analyzed by TaqMan gene expression assay. Relative expression was calculated via the comparative C_T method using the small nucleolar RNA transcript RNU44 (for microRNA analysis) or beta-glucuronidase (*BGUS*: for *ATM* analysis) as internal references (22). Quantitative reverse transcription-polymerase chain reactions (qRT-PCR) without reverse transcriptase were carried out in parallel for each RNA sample to exclude signal by contaminating genomic DNA.

Gene expression profiling

The retroviral clones with mi-RNA genes miR-181a, miR-323, miR-326, miR-342, miR-345 and miR-371, and negative control miR-Vec-Ctrl were transiently transfected in VU-SCC-120 by FuGENE 6 (Roche Diagnostics). Total RNA was isolated 72 hours after transfection using the mirVana mi-RNA Isolation Kit (Ambion). Microarray hybridization using the Agilent Low Input Quick Amplification Labeling Kit and 4 × 44K Whole Human Genome Arrays was carried out according to the manufacturer (Agilent Technologies). Normalization of the gene expression data was conducted within the R statistical software using the Limma package and comprised RMA background correction, loess within-array normalization, and A-quantile between-array normalization. Then, missing values were imputed using the impute-package (impute.knn with default settings). Finally, the slide and dye effects were removed by gene-wise linear regression using the log intensity values.

The log fold changes between the reference group and each treated group were used to cluster the 6 treatments. This was carried out by means of hierarchical clustering with ward linkage, and the similarity defined both as the Euclidean distance and as one minus the absolute value of the Spearman rank correlation measure. The grouping from hierarchical clustering was verified by means of principal component plots. Within each cluster, the differences in gene expression between reference and treated samples were evaluated by means of a *t* test. The multiplicity problem (many genes were tested) was addressed by application of the Benjamini-Hochberg procedure to the raw *P* values to control the false discovery rate (FDR). Data are accessible under GEO number GSE34881.

ATM inhibitor treatment

Both ciOKC and VU-SCC-120 cells were subjected to a concentration range of 40 to 0.075 µmol/L ATM inhibitor CP466722 (Axon Medchem). After 72 hours, cell viability was assessed with the CellTiter-Blue Cell Viability Assay.

ATM 3'UTR luciferase reporter assay

CiOKC cells were transiently cotransfected with a luciferase reporter construct containing the 3'UTR sequence of *ATM* (GeneCopoeia Inc.) and one of the retroviral vectors containing the miR-181a, miR-323, miR-326 genes, or negative control miR-Vec-Ctrl by FuGENE 6. In total 72 hours after transfection, firefly and *Renilla* luciferase activity was measured using the LucPair miR Dual Luciferase Assay Kit according to the instructions of the manufacturer (GeneCopoeia Inc.). Luciferase activity was measured using the Infinite 200 Plate Reader (Tecan Group Ltd.).

Lethal phenotype rescue

VU-SCC-120 cells were transiently transfected with either pcDNA3.1(+)-Flag-His-ATMwt (wild-type *ATM* cDNA sequence, Addgene plasmid 31985) or pcDNA3.1(+)-Flag-His-ATMkd (kinase-dead *ATM* cDNA sequence, Addgene plasmid 31986; ref. 23). Amphotropic retroviral supernatants were produced for miR-181a, miR-326, miR-345, and miR-Vec-Ctrl (scrambled sequence) as negative control. VU-SCC-120-ATMwt and VU-SCC-120-ATMkd cells were transduced with the microRNA expressing retroviruses at 2 following days for 4 hours in the presence of 3 µg/mL polybrene. After 72 hours, cell viability was assessed by the CellTiter-Blue Cell Viability Assay.

Results

Identification of mi-RNAs lethal for HNSCCs

To identify mi-RNAs that are lethal for head and neck cancer cells, we introduced a human mi-RNA expression library (miR-Lib) in HNSCC cell line VU-SCC-120 and close to normal ciOKCs (Fig. 1A). The ciOKC cells have been immortalized by a temperature-sensitive SV40 large T antigen. When cultured at 32°C, they are immortalized, while they become senescent when shifted to 39°C as a result of the inactivation of the large T-antigen. They behave, also at

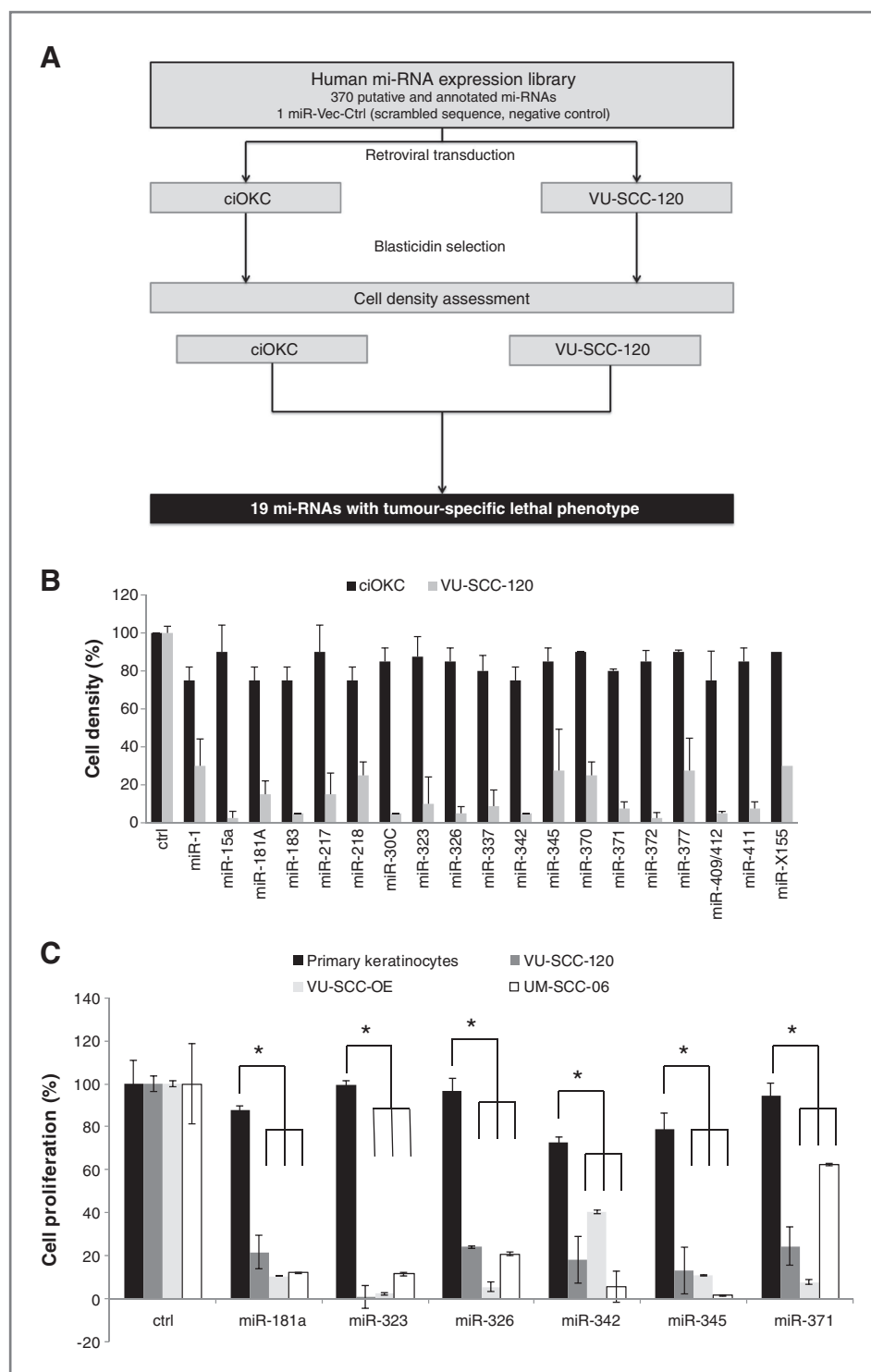


Figure 1. Identification of 19 mi-RNAs with a potential tumor-specific lethal effect by a functional genetic screen. **A**, schematic representation of the primary tumor-specific lethality screen. Both ciOKC and VU-SCC-120 cells were retrovirally transduced with a human mi-RNA expression library. After blasticidin selection of transduced cells, cell density was assessed. The mi-RNAs that had little to no effect on cell density (70%–100%) in ciOKC cells but did result in low cell density (0%–30%) in VU-SCC-120 cells were identified as potentially tumor-specific lethal. **B**, the 19 mi-RNAs that were selected in the initial screen showed cell survival differences between ciOKC (dark gray bars) and VU-SCC-120 (gray bars) cells. Cell density in duplicate wells was visually estimated by two independent observers, with standard deviations (SDs) as error bars. **C**, the effect of ectopic expression of the indicated 6 mi-RNAs on survival of primary oral keratinocytes (dark gray bars) and head and neck cancer cell lines VU-SCC-120 (medium gray bars), VU-SCC-OE (light gray bars), and UM-SCC-6 (very light gray bars). Cell proliferation was quantified by the CellTiter-Blue Assay. The average value of triplicate experiments is shown, with SDs as error bars. Significant differences are indicated by an * ($P < 0.05$, Student *t* test).

32°C, as normal keratinocytes except for the immortalized phenotype (18).

The majority of mi-RNAs did not influence the survival of either tumor cells or ciOKC cells, or the lethal effect was similar in both models. However, a subset of 19 mi-RNAs (5.4%) specifically affected the head and neck cancer cell line,

whereas the ciOKCs remained unaffected (Supplementary Table S1; Fig. 1B). To verify the tumor-specific lethal effect of these mi-RNAs, we screened all 19 mi-RNAs in 2 different ciOKC cell clones and 3 HNSCC cell lines (VU-SCC-OE, UM-SCC-6, and VU-SCC-120). We could not confirm the tumor-specific lethal effect of thirteen mi-RNAs. The

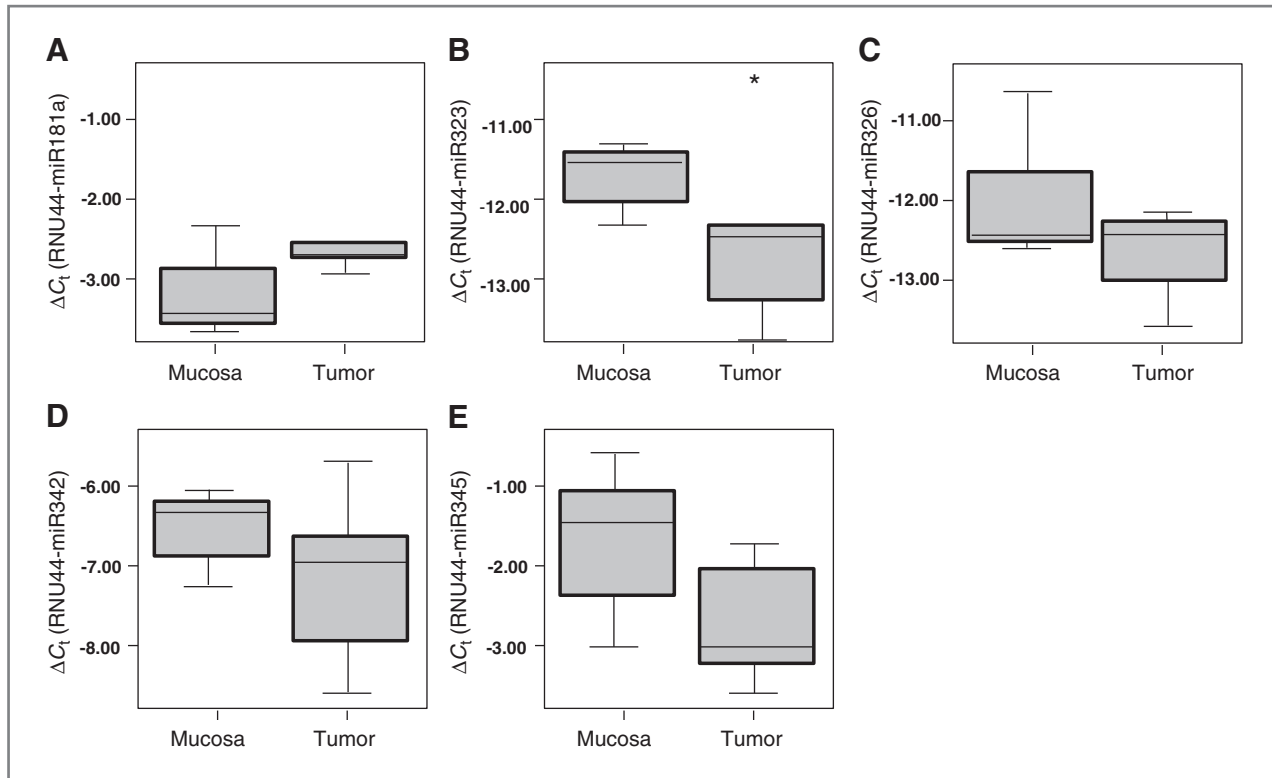


Figure 2. Box plots of the expression of the six lethal mi-RNAs in HNSCC tumors and normal mucosal epithelium. mi-RNA levels were determined using qRT-PCR analysis on RNA of microdissected FFPE tumors and mucosal epithelium. ΔC_T values, $C_T(\text{mi-RNA}) - C_T(\text{RNU44})$, are depicted for (A) miR-181a, (B) miR-323, (C) miR-326, (D) miR-342, and (E) miR-345. MiR-371 was not expressed in squamous tissues. Significant differences are indicated by an asterisk ($P < 0.05$ with Student *t* test).

remaining 6 mi-RNAs showed the expected phenotype (Supplementary Fig. S1): a decreased proliferation in HNSCC cells but not in ciOKC cells and these mi-RNAs were further investigated. Visual inspection indicated that the tumor cells had disappeared from the wells indicating that they likely ceased proliferation and died. As yet, we did not elucidate the precise molecular mechanism behind the cell death.

For the initial large scale discovery screens, we had to rely on the ciOKC cell model to study the effect of the mi-RNAs. In the subsequent small-scale validation experiments we included primary keratinocytes. The mi-RNAs miR-181a, miR-323, miR-326, miR-342, miR-345, and miR-371 all showed a significant decrease in cell proliferation in 3 HNSCC cell lines and not or only to a limited extent in primary keratinocytes (Fig. 1C). The sequence identity of these 6 mi-RNAs was confirmed by Sanger sequencing (data not shown).

mi-RNA expression in HNSCCs

As the ectopic expression of the 6 tumor-selective lethal mi-RNAs caused cell death in tumor cell lines but not or less in mucosal keratinocytes, we were interested in the expression of these mi-RNAs in HNSCC tumors and normal oral mucosa. Hence, we determined expression levels for the 6 mi-RNAs in RNA extracted from both microdissected tumor and mucosal epithelium. miR-371 was neither expressed in normal mucosa nor in the 5 tumors analyzed (data not

shown). For the other 5 mi-RNAs, expression was observed in all tumor and mucosal epithelium samples but apparently at a low level (Fig. 2). The expression levels of the mi-RNAs were in all cases lower than the expression of the *RNU44* reference gene. In addition, only small differences in expression levels were observed between mucosa and tumor samples. The expression of miR-181a was slightly increased in tumors but not significant (Fig. 2A). For miR-326, miR-342, and miR-345, the expression level in tumor tissue was decreased when compared to normal mucosal epithelium but not significantly. Only the expression level of miR-323 was significantly lower in tumor cells (Fig. 2B).

Tumor-specific lethal phenotype in cell lines of different cancer types

We next questioned whether the effect observed in the HNSCC cell lines was specific for HNSCCs. Therefore, we tested the 6 mi-RNAs with HNSCC-specific lethal effects in other cancer cell lines. The introduction of the various mi-RNAs in cervical carcinoma cell line (SiHa) and breast carcinoma cell line (MCF7) had no effect on proliferation except for mi-RNA 181a (Supplementary Fig. S2A and S2B). However, when the mi-RNAs were introduced in colon adenocarcinoma cell line (HT29) or glioblastoma cell line (U87), a decrease in cell proliferation was observed, although with a less severe phenotype than the tested

HNSCC cell lines (Supplementary Fig. S2C and S2D). The effects observed vary with the specific microRNA. This strongly suggests that genes are targeted that show synthetic lethal interactions in relation to the mutational status of specific cancer genes or deregulated signaling pathways in the various cell lines of different tissue origin, and it might be worthwhile to repeat these functional screens for other tumor types as it might reveal other candidate microRNAs. The lethal interaction is likely not related to a mutation in *TP53* as all mi-RNAs showed the tumor-selective lethal effect in all 3 HNSCC cell lines, whereas one cell line was *TP53* wild-type, one showed two missense mutations, and one a large deletion (see Materials and Methods for details).

Target gene analysis

mi-RNAs regulate gene expression at the posttranscriptional level, so we were interested in the downstream gene targets of these 6 tumor-specific lethal mi-RNAs that might explain the cell growth inhibitory phenotype. First, we conducted an *in silico* analysis. There is a multitude of software tools available for target identification (reviewed

in ref. 24), and we chose TargetScan and DIANA-microT. We also defined the overlap between genes detected by the 2 programs (Supplementary Table S4). There was a wide variety of potential genes identified with more than 700 for miR-181a. This analysis did not give a direct clue.

Therefore, we conducted microarray-based gene expression analysis to identify candidate target genes. As ectopic expression of these mi-RNAs caused a decrease in cell proliferation and cell death as phenotype in HNSCC cell lines, we were unable to analyze cells stably transduced with the mi-RNAs. We therefore decided to transiently transfect VU-SCC-120 cells with the retroviral vector plasmids instead of transduction with retroviral particles. Transient transfection is efficient, and overexpression can be observed almost immediately. RNA was isolated 72 hours posttransfection, the time point with high mi-RNA expression, but before cell death was observed (Supplementary Fig. S3). The expression level of the transfected mi-RNAs was also determined. Depending on the endogenous expression of the mi-RNAs in VU-SCC-120 cells, expression increased from 23- to 4,000-fold after transient transfection (Fig. 3A and B).

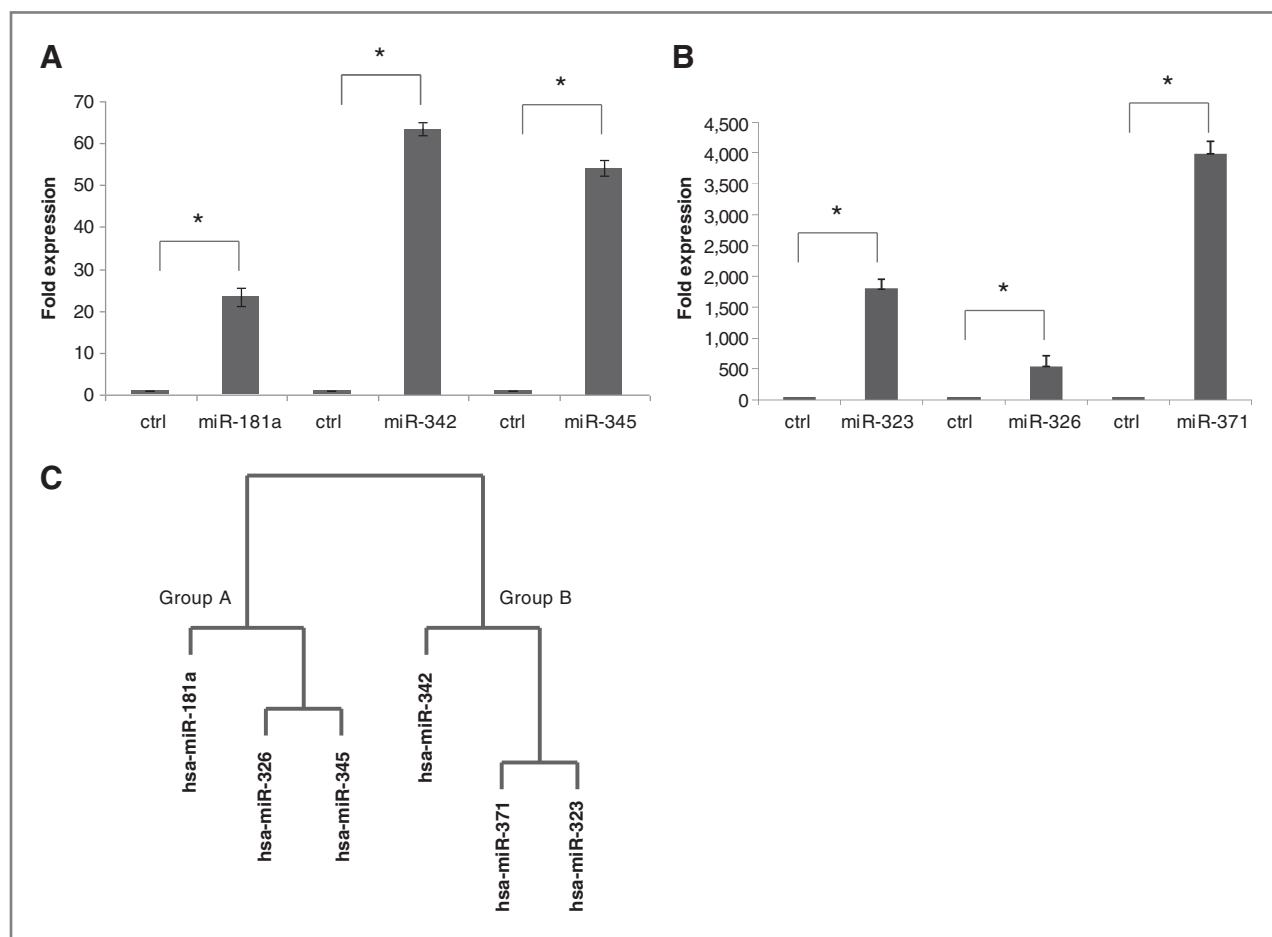


Figure 3. Ectopic expression of mi-RNAs and their effect on gene expression. VU-SCC-120 cells were transiently transfected with the six different mi-RNA plasmids and overexpression of the indicated mi-RNAs was compared with miR-Vec-Ctrl-transfected cells for (A) miR-181a, miR-326, and miR-345 as well as (B) miR-323, miR-326, and miR-371. Significant differences are indicated by an * ($P < 0.05$, Student *t* test). Two separate groups became apparent by hierarchical cluster analysis (C).

Table 1. Correlations of gene expression profiles between different microRNAs

	miR-181a	miR-326	miR-371	miR-345	miR-323	miR-342
miR-181a	1.000					
miR-326	0.572	1.000				
miR-371	0.113	0.119	1.000			
miR-345	0.373	0.573	0.158	1.000		
miR-323	0.099	0.087	0.602	0.170	1.000	
miR-342	0.074	0.065	0.388	0.123	0.577	1.000

Next, total RNA of the transfected cells was labeled and hybridized for gene expression profiling by microarray hybridization. We assumed that some of these 6 mi-RNAs might in fact target the same genes, and we therefore focused on a groupwise comparison. In the expression profiles, we indeed observed significant correlations between miRNA-associated mRNA expression profiles (Table 1). Highly significant correlations were observed for miR-181a and miR-326 ($r = 0.572$), miR-326 and miR-345 ($r = 0.573$), miR-323 and miR-371 ($r = 0.602$), and miR-342 and miR-323 ($r = 0.577$). Cluster analysis revealed 2 groups of each 3 miRNAs with downstream target effects that showed significant correlations (Fig. 3C; Supplementary Tables S2 and S3). miR-181a, miR-326, and miR-345 clustered together in group A, and group B was composed of miR-342, miR-371 and miR-323. The profiles of the mi-RNAs per group were combined and analyzed against the empty vector control (in tetraplicate hybridized on the arrays) to detect significant differentially expressed genes.

In total, we observed 187 and 15 genes (FDR-corrected P value < 0.1) that were significantly differentially expressed between groups A and B, respectively, as compared to the empty vector control. Subsequently, we applied several rankings on the differentially expressed genes to distinguish primary effects from secondary effects. First, we ranked the genes for a decreased level of expression, as mi-RNAs are considered to cause downregulation of expression of their target genes. Second, as for many genes multiple probes were present on the array, we subsequently ranked the genes for the number of probes per gene with an FDR-corrected P value < 0.1 (Supplementary Tables S2 and S3). One of the most striking target genes that is apparently regulated by the mi-RNAs from group A is the *ATM* gene. First, the differences of many probes were highly significant given the limited sample size (4 controls vs. 3 mi-RNAs of group A analyzed in duplicate) and the conservative P value adjustment. Second, in total 9 of 12 *ATM* probes were significantly regulated. Unfortunately, we did not find such an apparent lead target for the miRNAs in group B.

Knockdown of ATM causes tumor-specific lethality

ATM is a nuclear protein kinase that senses DNA damage and activates downstream pathways (24). To validate the observed decrease in expression, we carried out qRT-PCR for *ATM* in the same samples that were transiently transfected with the mi-RNAs and that were

analyzed by microarray hybridization. Indeed we confirmed that *ATM* expression is inhibited in the RNA samples from group A (Fig. 4A).

As ectopic expression of miR-181a, miR-326, and miR-345 results in tumor-specific lethality and downregulation of *ATM* expression, we hypothesized that knockdown of *ATM* may also be accompanied by tumor-specific lethality in HNSCC cells. Therefore, we introduced 5 lentiviral shRNA constructs designed to specifically knockdown *ATM* expression in ciOKC cells and VU-SCC-120. Each shRNA sequence was complementary to a unique part of the *ATM* mRNA sequence. Introduction of the *ATM* shRNAs resulted in a minor inhibition of cell proliferation in ciOKC cells compared with cells transduced with a control construct (ctrl), but proliferation was significantly inhibited in HNSCC cell line VU-SCC-120, ranging from 21% to 90% (Fig. 4B). The maximum window was observed with shRNA *ATM1*. It was at least 8 times more active in the tumor cell line as compared to the ciOKC cells. To check the knockdown, *ATM* expression was analyzed by qRT-PCR and expression levels were compared with the cells transduced with the control construct. Introduction of 4 of 5 *ATM* shRNAs resulted in more than 70% downregulation of *ATM* expression levels. Only transduction with *ATM* shRNA number 5 did not result in significant downregulation of *ATM* expression (Fig. 4C).

ATM is a kinase and druggable by kinase inhibitors. To confirm the tumor-specific decrease in cell viability by *ATM* inhibition, we also subjected ciOKC and HNSCC cells to different concentrations of the commercially available specific *ATM* inhibitor CP466722. Analysis of cell viability showed that HNSCC cells were more sensitive to the inhibitor compared to the ciOKC cells (Fig. 4D). The IC_{50} of 8.2 $\mu\text{mol/L}$ in ciOKC cells shifts to 2.6 $\mu\text{mol/L}$ in VU-SCC-120, a significant change of 3-fold ($P < 0.05$ by t testing).

Inhibition of *ATM* by microRNA overexpression, specific *ATM* shRNAs, or kinase inhibitors results in a decrease in cell proliferation in HNSCC cells. When *ATM* is the direct effector, ectopic expression of *ATM* should rescue the HNSCC cells from cell death. To investigate this, VU-SCC-120 cells were transfected with either wild-type *ATM* (*ATMwt*) or a kinase-dead mutant *ATM* (*ATMkd*) in an expression cassette that lacks the 3'UTR of *ATM*. Overexpression of *ATMwt* or *ATMkd* was confirmed by qRT-PCR (Supplementary Fig. S4). Next mi-RNAs, miR-181a, miR-326, and miR-345 were introduced in these two cell lines and compared with

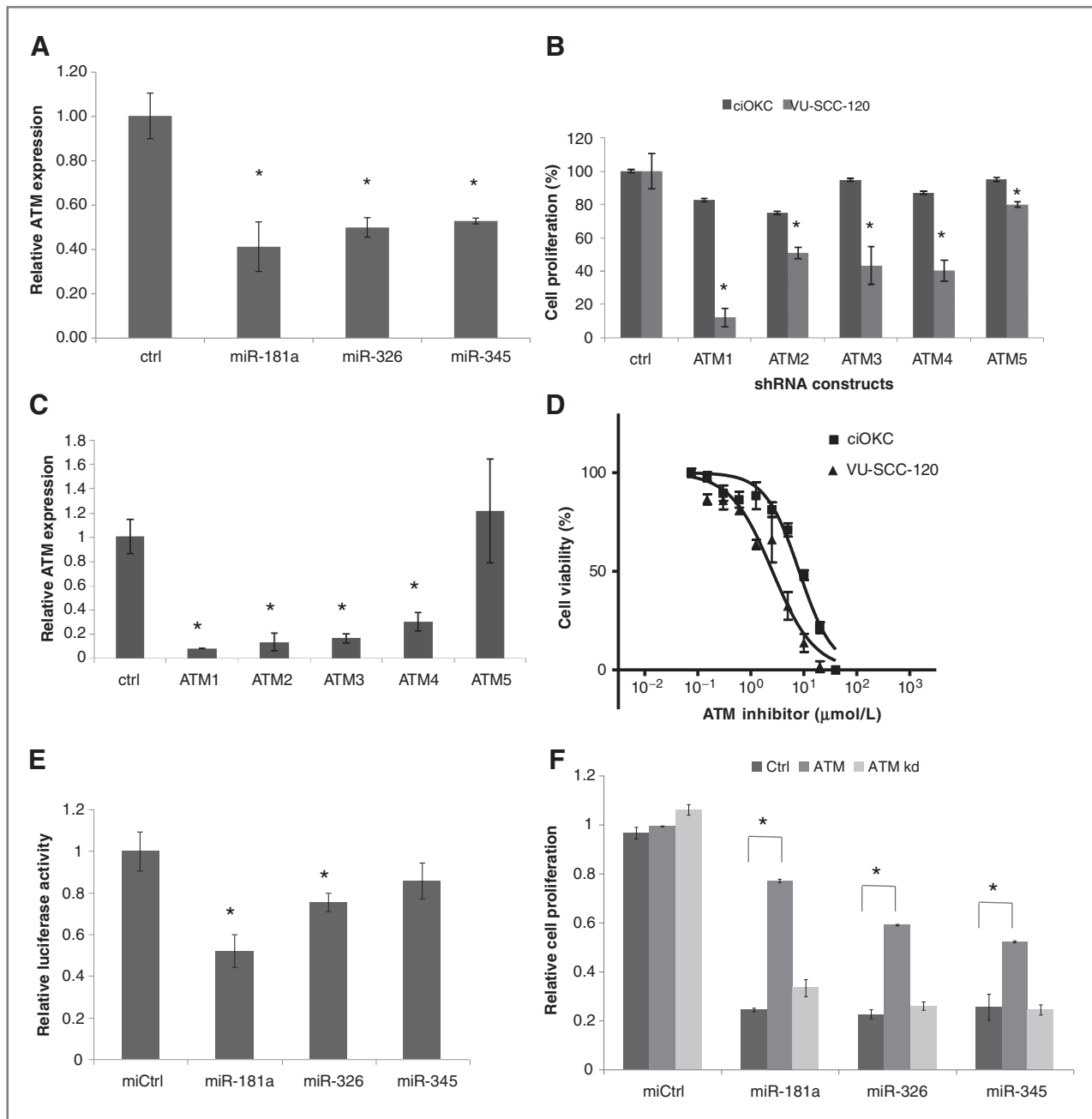


Figure 4. *ATM* expression is regulated by miR-181a, miR-326, and miR-345 from group A. **A**, endogenous *ATM* expression in ciOKC cells was analyzed by qRT-PCR after transient transfection with miR-Vec-Ctrl or the miRNA constructs indicated. In **(B)**, cell proliferation of ciOKC (dark gray bars) and VU-SCC-120 (medium gray bars) is depicted after *ATM* knockdown with 5 different shRNA constructs and control vector (ctrl). In **(C)**, the knockdown of endogenous *ATM* expression in ciOKC cells is depicted after lentiviral transduction with either a control construct (ctrl) or *ATM* shRNA constructs 1 to 5. In **(D)**, sensitivity of HNSCC cell lines VU-SCC-120 and ciOKC cells to the *ATM* drug CP466722 is determined. In **(E)** the effect of the miRNAs of group A on the *ATM* 3'UTR luciferase reporter construct is shown. The 3'UTR of *ATM* was cloned behind the firefly luciferase. Firefly luciferase activity was normalized using *Renilla* luciferase activity to correct for transfection efficiency. In **(F)** rescue experiments with *ATM* encoding expression constructs are depicted. Wild-type *ATM* (*ATM*; medium gray bars) or kinase-dead *ATM* (*ATMkd*; light gray bars) were transfected and the effect on the tumor-selective phenotype of miR-181a, miR-326, miR-345, or miR-Vec-Ctrl (miCtrl) compared with untransfected cells (ctrl; dark gray bars). The average of triplicate experiments is shown with standard deviations as error bars. Significant differences are indicated with an * ($P < 0.05$, Student *t* test).

untransduced VU-SCC-120 (ctrl). The mi-RNAs all showed a decrease in cell proliferation in the untransduced VU-SCC-120 (Fig. 4F). However, in the cells with the *ATM*_wt expression construct, cell proliferation was rescued up to about 50%

(miR-181a) and about 50% (miR-326 and miR-345). Rescue was not observed when the kinase-dead mutant *ATM* was ectopically expressed in VU-SCC-120 cells. These data indicate that the miRNAs inhibit *ATM* expression, which elicits

the tumor-selective lethal phenotype and it depends on the kinase activity of ATM.

Targeting of ATM by miR-181a, miR-326-, and miR-345

mi-RNAs are known to regulate gene expression posttranscriptionally via binding to the 3'UTR or coding sequences of an mRNA sequence. To show an effect of miR-181a, miR-326, and miR-345 on the 3'UTR of the *ATM* gene mi-RNAs were cotransfected with a luciferase reporter construct cloned to the *ATM* 3'UTR sequence. Transfection of ciOKCs with miR-181a and miR-326 suppressed the activity of a luciferase reporter gene cloned to the 3'UTR of *ATM*. miR-345 did show an effect but not significant (Fig. 4E).

The knockdown of *ATM* by the respective microRNAs seems to inversely correlate with the effect of ectopic *ATM* expression. In addition, ectopic *ATM* expression does not rescue the lethal phenotype to 100%. This suggests that some mi-RNAs might not target only the 3'UTR but also the 5'UTR or coding sequences. These sequences are still present in the expression construct, only the 3'UTR of *ATM* has been substituted. We further hypothesized that another gene target might be involved as well. First, we re-inspected our expression data and found another gene significantly down-regulated in 9 of 10 available probes: *CD40*. We next checked the presence of microRNA target sites using RNA22 and TargetScan on both *ATM* and *CD40*. Multiple binding sites were found for these microRNAs in these genes, albeit mostly not in the 3'UTR region (Supplementary Fig. S5). The relevance of the various putative mi-RNA target sites and the role of *CD40* and its interaction with *ATM* requires further elucidation.

Discussion

In the present study, we identified 6 mi-RNAs that, when ectopically expressed, lead to a tumor-specific inhibition of proliferation in HNSCC cells and not in primary keratinocytes. mi-RNAs are generally classified into different families based on their sequence homology, most particularly of the seed sequence, and it is hypothesized that different mi-RNAs within the same family may have similar effects on gene expression. Although all mi-RNAs highlighted in this study have a tumor-specific lethal effect, and some even recognize at least one identical and apparently critical target gene, they do not belong to the same family.

Many mi-RNAs have already been implicated in cancer development and progression. For miR-345, a role in head and neck cancer development has been suggested previously by profiling studies. In these studies, mi-RNA expression profiles in tumor samples were compared with normal mucosal epithelium, and it was shown that miR-345 showed an increased expression level in malignant cells (10). miR-181a has been shown by functional studies to have tumor-suppressive properties in HNSCCs (15). Here, we show a tumor-specific lethal effect for ectopic expression of these 2 miRs as well as miR-326, miR-342, miR-371, and miR-323 in head and neck cancer cells. We also show that a similar lethal effect was observed when those 6 mi-RNAs

were introduced in colon cancer and glioblastoma cell lines, although there was a considerable variation in the lethal phenotype between cell lines of different origin. It might therefore be of interest to repeat similar screens in other tumor types. Unfortunately, it is not always possible to have access to matched normal (or near normal) cells, which are required to allow a tumor-specific lethal screen and subsequent validation. Assuming that the identified hits are synthetic lethal with cancer-associated alterations in conserved cellular pathways such as cell-cycle control or DNA repair, the precise source and histotype of the normal reference cells might be less critical, and normal fibroblasts may be sufficient.

mi-RNAs regulate gene expression at the posttranscriptional level. One gene may be regulated by multiple mi-RNAs but also one mi-RNA may regulate multiple genes. Consequently, it is difficult to study downstream targets of a certain mi-RNA, particularly as the target genes may also be involved in the regulation of expression of other genes. Therefore, it is not surprising that many genes were shown to be significantly differentially expressed when the effect of the 6 tumor-specific lethal mi-RNAs was analyzed. Although the expression profiles of the 6 mi-RNAs were not similar, it was interesting to observe that 2 groups could be discriminated. Unfortunately, we could not identify an apparent candidate target gene in group B. Likely multiple repeats of the array analysis in multiple cell lines will be required to define more convincing candidate target genes. The limited sample size combined with the strict FDR correction of the *P* values may have skewed the analyses. Moreover, mi-RNAs might also influence genes at the translational level, which would necessitate alternative approaches to identify the candidate target genes.

However, in group A, several probes for *ATM* showed significant differences. Using *ATM* 3'UTR luciferase reporter experiments, we showed that both miR-181a and miR-326 seem to directly target the 3'UTR sequence of *ATM*. We could not confirm this for miR-345. We also showed that specific downregulation of *ATM* via shRNA knockdown elicits a similar tumor-specific lethal phenotype. Although there was a slight toxic effect in the normal squamous epithelial cells, the lethal phenotype observed in HNSCC cell lines was much more severe, and HNSCC cells are more sensitive to the specific *ATM* inhibitor CP466722. Finally, the tumor-selective phenotype of the mi-RNAs could be rescued by introduction of an *ATM* expression construct that lacks the 3'UTR of *ATM* itself, whereas the phenotype could not be rescued by expression of a kinase-dead mutant.

Intriguingly, there seemed an inverse correlation between reduction of luciferase activity with the *ATM* 3'UTR and the rescue level when expressing an *ATM* cDNA sequence without the 3'UTR, strongly suggesting that target sites in the coding cDNA sequence are highly relevant as well. When analyzing the potential target sites by RNA22 and TargetScan, a binding site for miR-181a was found in the 3'UTR of *ATM*, but many more in the coding cDNA sequence. Mutation of predicted target sites will be required to proof the relevance of all of them, which will be a major future task. A

worrying observation is that the various prediction programs come up with different potential binding sites, hampering a focused approach. Nonetheless, such experiments will be required to establish the ultimate proof of *ATM* targeting by the microRNAs of group A.

We also observed that the rescue level never reaches 100% cell survival. There might be many explanations for this observation, but it suggests that also another target gene might be involved, and we could pinpoint CD40 as a first hint. Additional experiments will be required to prove this and that combined targeted treatment might be of benefit.

Our data thus far suggest that HNSCC cells are depending on *ATM* signaling for their survival. When *ATM* expression is lost, either by shRNA knockdown or when targeted by an mi-RNA, the cell is unable to survive, at least under culture conditions. *ATM* senses DNA damage and phosphorylates CHEK2 which in turn activates p53 by phosphorylation. This route plays a major role in maintaining genome integrity and cell-cycle control (25). Intriguingly, *TP53* is mutated in 2 of the 3 HNSCC cell lines tested and *ATM* may have become more critical to organize DNA repair or induce a cell-cycle block during S-G₂ phase after DNA damage independent of p53. The third cell line UM-SCC-6 is *TP53* wild-type but it is unclear whether p53 is still functionally active. Detailed analyses of the *ATM*/*ATR*-*CHEK1*/*CHEK2* pathway should reveal which critical downstream signaling route causes the lethal phenotype and what the mechanism is. Obviously *ATM* has many downstream targets, and the tumor-selective phenotype might be related to alterations in other signaling routes. Nonetheless, our data suggest that *ATM* is an interesting drug target for HNSCCs.

Previously, it has been shown that miR-181a targets *KRAS*, and this was put forward as explanation that this particular microRNA inhibits proliferation of squamous cancer cells (15). This seemed a little remarkable as *KRAS* mutations are hardly found in HNSCCs, suggesting that this is not the most critical driving gene or even pathway in squamous oncogenesis. On the basis of our data, we assume that the targeting of *ATM* by miR-181a is the likely event that causes a proliferation stop and cell death in squamous cancer cells.

In summary, we show here that functional screens by microRNA expression libraries are an effective way to identify novel druggable targets. We showed that the ectopic

expression of mi-RNAs such as miR-323, miR-345, miR-371, miR-181a, miR-342, and miR-326 may serve as a new treatment in HNSCCs. Particularly in head and neck cancer where access to the tumor is relatively easy, introduction of mi-RNAs, for instance by intratumoral injection combined with electroporation, may be a therapeutic possibility in the future (26). Also, the application of *ATM* inhibiting drugs might be a very interesting approach to study in clinical trials specifically focusing on HNSCCs.

Disclosure of Potential Conflicts of Interest

R.H. Brakenhoff has a commercial research grant from InteRNA Technologies BV. InteRNA Technologies BV has filed a patent application regarding the inventions described in this manuscript. No potential conflicts of interest were disclosed by the other authors.

Authors' Contributions

Conception and design: M. Lindenbergh-van der Plas, S.R. Martens-de Kemp, C.R. Leemans, B.J.M. Braakhuis, R.H. Brakenhoff

Development of methodology: M. Lindenbergh-van der Plas, S.R. Martens-de Kemp, R. Agami, R.H. Brakenhoff

Acquisition of data (provided animals, acquired and managed patients, provided facilities, etc.): M. Lindenbergh-van der Plas, S.R. Martens-de Kemp, B. Ylstra, R.H. Brakenhoff

Analysis and interpretation of data (e.g., statistical analysis, biostatistics, computational analysis): M. Lindenbergh-van der Plas, S.R. Martens-de Kemp, W.N. van Wieringen, F. Cerisoli, C.R. Leemans, B.J.M. Braakhuis, R.H. Brakenhoff

Writing, review, and/or revision of the manuscript: M. Lindenbergh-van der Plas, S.R. Martens-de Kemp, B. Ylstra, F. Cerisoli, C.R. Leemans, B.J.M. Braakhuis, R.H. Brakenhoff

Administrative, technical, or material support (i.e., reporting or organizing data, constructing databases): M. Lindenbergh-van der Plas, M. de Maaker, R.H. Brakenhoff

Study supervision: R.H. Brakenhoff

Acknowledgments

The authors thank Patrizia Rizzu and Peter Heutink for providing the *ATM* shRNA clones; Thomas Carey for providing the UM-SCC-6 cell line; Francois Rustenburg for carrying out the microarray hybridizations; and René Bernards and Katrien Berns for help with the generation of the cIOCK model.

Grant Support

The authors thank InteRNA Technologies BV and VUmc Cancer Center Amsterdam for financial support.

The costs of publication of this article were defrayed in part by the payment of page charges. This article must therefore be hereby marked *advertisement* in accordance with 18 U.S.C. Section 1734 solely to indicate this fact.

Received July 19, 2012; revised May 30, 2013; accepted July 19, 2013; published OnlineFirst August 13, 2013.

References

- Leemans CR, Braakhuis BJM, Brakenhoff RH. The molecular biology of head and neck cancer. *Nat Rev Cancer* 2011;11:9–22.
- Parkin DM, Bray F, Ferlay J, Pisani P. Global cancer statistics, 2002. *CA Cancer J Clin* 2005;55:74–108.
- Braakhuis BJM, Snijders PJF, Keune WJH, Meijer CJLM, Ruijter-Schippers HJ, Leemans CR, et al. Genetic patterns in head and neck cancers that contain or lack transcriptionally active human papillomavirus. *J Natl Cancer Inst* 2004;96:998–1006.
- Gillison ML, Koch WM, Capone RB, Spafford M, Westra WH, Wu L, et al. Evidence for a causal association between human papillomavirus and a subset of head and neck cancers. *J Natl Cancer Inst* 2000;92:709–20.
- van Houten VMM, Snijders PJF, van den Brekel MWM, Kummer JA, Meijer CJLM, van Leeuwen B, et al. Biological evidence that human papillomaviruses are etiologically involved in a subgroup of head and neck squamous cell carcinomas. *Int J Cancer* 2001;93:232–5.
- Cho WCS. OncomiRs: the discovery and progress of microRNAs in cancers. *Mol Cancer* 2007;6:60.
- Salmerna L, Poliseno L, Tay Y, Kats L, Pandolfi PP. A ceRNA Hypothesis: the Rosetta stone of a hidden RNA language? *Cell* 2011;146:353–8.
- Fabian MR, Sonenberg N, Filipowicz W. Regulation of mRNA Translation and stability by microRNAs. *Annu Rev Biochem* 2010;79:351–79.

9. Baek D, Villen J, Shin C, Camargo FD, Gygi SP, Bartel DP. The impact of microRNAs on protein output. *Nature* 2008;455:64–U38.
10. Cervigne NK, Reis PP, Machado J, Sadikovic B, Bradley G, Galloni NN, et al. Identification of a microRNA signature associated with progression of leukoplakia to oral carcinoma. *Hum Mol Genet* 2009;18:4818–29.
11. Ramdas L, Giri U, Ashorn CL, Coombes KR, El Naggar A, Ang KK, et al. MiRNA expression profiles in head and neck squamous cell carcinoma and adjacent normal tissue. *Head Neck* 2009;31:642–54.
12. Chang KW, Liu CJ, Chu TH, Cheng HW, Hung PS, Hu WY, et al. Association between High miR-211 microRNA expression and the poor prognosis of oral carcinoma. *J Dent Res* 2008;87:1063–8.
13. Li JS, Huang HZ, Sun LJ, Yang M, Pan CB, Chen WL, et al. MiR-21 indicates poor prognosis in tongue squamous cell carcinomas as an apoptosis inhibitor. *Clin Cancer Res* 2009;15:3998–4008.
14. Cimmino A, Calin GA, Fabbri M, Iorio MV, Ferracin M, Shimizu M, et al. MiR-15 and miR-16 induce apoptosis by targeting BCL2. *Proc Natl Acad Sci USA* 2005;102:13944–9.
15. Shin KH, Bae SD, Hong HS, Kim RH, Kang MK, Park NH. MiR-181a shows tumor suppressive effect against oral squamous cell carcinoma cells by downregulating K-ras. *Biochem Biophys Res Commun* 2011;404:896–902.
16. Guo GS, Zhang FM, Gao RJ, Delsite R, Feng ZH, Powell SN. DNA repair and synthetic lethality. *Int J Oral Sci* 2011;3:176–9.
17. Van Zeeburg HJT, van Beusechem VW, Huizenga A, Haisma HJ, Korokhov N, Gibbs S, et al. Adenovirus retargeting to surface expressed antigens on oral mucosa. *J Gene Med* 2010;12:365–76.
18. Smeets SJ, van der Plas M, Schaaij-Visser TBM, van Veen EAM, van Meerloo J, Braakhuis BJM, et al. Immortalization of oral keratinocytes by functional inactivation of the p53 and pRb pathways. *Int J Cancer* 2011;128:1596–605.
19. Voorhoeve PM, Le Sage C, Schrier M, Gillis AJM, Stoop H, Nagel CR, et al. A genetic screen implicates miRNA-372 and miRNA-373 as oncogenes in testicular germ cell tumors. *Cell* 2006;124:1169–81.
20. Hermesen MAJA, Joenje H, Arwert F, Welters MJP, Braakhuis BJM, Bagnay M, et al. Centromeric breakage as a major cause of cytogenetic abnormalities in oral squamous cell carcinoma. *Genes Chromosomes Cancer* 1996;15:1–9.
21. Bremner JF, Braakhuis BJM, Ruijter-Schippers HJ, Brink A, Duarte HMB, Kuik DJ, et al. A noninvasive genetic screening test to detect oral preneoplastic lesions. *Lab Invest* 2005;85:1481–8.
22. Schmittgen TD, Livak KJ. Analyzing real-time PCR data by the comparative C-T method. *Nature Prot* 2008;3:1101–8.
23. Canman CE, Lim DS, Cimprich KA, Taya Y, Tamai K, Sakaguchi K, et al. Activation of the ATM kinase by ionizing radiation and phosphorylation of p53. *Science* 1998;281:1677–9.
24. Witkos TM, Koscianska E, Krzyzosiak WJ. Practical aspects of micro-RNA target prediction. *Curr Mol Med* 2011;11:93–109.
25. Shiloh Y. ATM and related protein kinases: safeguarding genome integrity. *Nat Rev Cancer* 2003;3:155–68.
26. Takei Y, Nemoto T, Mu P, Fujishima T, Ishimoto T, Hayakawa Y, et al. In vivo silencing of a molecular target by short interfering RNA electroporation: tumor vascularization correlates to delivery efficiency. *Mol Cancer Ther* 2008;7:211–21.